Elevated ERK/p90 ribosomal S6 kinase activity underlies audiogenic seizure susceptibility in fragile X mice

Kirsty Sawicka[a,1,2,3], Alexander Pyronneau[a,1], Miranda Chao[a], Michael V. L. Bennett[a,3], and R. Suzanne Zukin[a,3]

[a]Dominick P. Purpura Department of Neuroscience, Albert Einstein College of Medicine, New York, NY 10461

Contributed by Michael V. L. Bennett, August 8, 2016 (sent for review June 24, 2016; reviewed by Leonard K. Kaczmarek and Siqiong June Liu)

Fragile X syndrome (FXS) is the most common heritable cause of intellectual disability and a leading genetic form of autism. The *Fmr1* KO mouse, a model of FXS, exhibits elevated translation in the hippocampus and the cortex. ERK (extracellular signal-regulated kinase) and mTOR (mechanistic target of rapamycin) signaling regulate protein synthesis by activating downstream targets critical to translation initiation and elongation and are known to contribute to hippocampal defects in fragile X. Here we show that the effect of loss of fragile X mental retardation protein (FMRP) on these pathways is brain region specific. In contrast to the hippocampus, ERK (but not mTOR) signaling is elevated in the neocortex of fragile X mice. Phosphorylation of ribosomal protein S6, typically a downstream target of mTOR, is elevated in the neocortex, despite normal mTOR activity. This is significant in that S6 phosphorylation facilitates translation, correlates with neuronal activation, and is altered in neurodevelopmental disorders. We show that in fragile X mice, S6 is regulated by ERK via the "alternative" S6 kinase p90-ribosomal S6 kinase (RSK), as evidenced by the site of elevated phosphorylation and the finding that ERK inhibition corrects elevated RSK and S6 activity. These findings indicate that signaling networks are altered in the neocortex of fragile X mice such that S6 phosphorylation receives aberrant input from ERK/RSK. Importantly, an RSK inhibitor reduces susceptibility to audiogenic seizures in fragile X mice. Our findings identify RSK as a therapeutic target for fragile X and suggest the therapeutic potential of drugs for the treatment of FXS may vary in a brain-region–specific manner.

intellectual disability | autism | mTOR | FMRP | RSK

Fragile X syndrome (FXS) is the most common heritable form of intellectual disability and a leading genetic cause of autism. Individuals with FXS typically suffer from a range of cognitive and behavioral deficits that can include anxiety, stereotypic movements, hyperactivity, seizures, and aggression, as well as social deficits typical of autism (1). FXS is caused by transcriptional silencing or mutation of the *FMR1* gene encoding the RNA-binding protein, FMRP (fragile X mental retardation protein). FMRP binds to >1,000 mRNAs, including transcripts encoding both pre- and postsynaptic proteins important for synaptic function, and represses their translation via ribosome stalling (2). Loss of FMRP expression in fragile X syndrome would be expected to cause translational derepression of these target mRNAs.

FMRP is strategically localized to dendrites, dendritic spines, axons, and cell bodies to control protein synthesis. Loss of FMRP causes enhanced protein synthesis, which can lead to altered spine morphology, synaptic circuits, and synaptic function with robust effects on higher cognitive function. The excessive, unchecked protein synthesis and impaired stimulus-induced protein synthesis are considered to be major contributors to the pathophysiology of fragile X (3–5). Increased protein synthesis has been demonstrated in whole-animal studies in fragile X mice (*Fmr1* KO) that model the loss of FMRP function responsible for the human disorder (6), brain slices from fragile X mice (7), and cell cultures from human subjects with fragile X (8). FMRP directly regulates the translation of a specific subset of target mRNAs. Given that these represent ∼5% of all mRNAs and are relatively low-abundance transcripts, the magnitude of the observed increase in global protein synthesis (∼15–20%) suggests that secondary effects on translation are also involved (9). Consistent with this finding, FMRP targets include components of ERK (extracellular signal-regulated kinase) and mTOR (mechanistic target of rapamycin) signaling and proteins involved in translation initiation and elongation (2).

PI3K/Akt/mTOR signaling is overactivated in the hippocampus of *Fmr1* KO mice (10, 11). Genetic and pharmacological interventions that reduce the activity of PI3-kinase (PI3K) or the downstream effector S6 kinase (S6K) have both shown promise for the rescue of disease-relevant phenotypes in the *Fmr1* KO mouse (12, 13). In contrast, ERK signaling appears normal in the hippocampus with no change in basal or activated levels of protein phosphorylation (10, 14). However, emerging evidence supports the concept that loss of FMRP can lead to synaptic defects that differ in an age-, synapse-, cell-, and/or brain region-specific manner as, for example, synapse-specific defects in synaptic plasticity (15), inhibitory circuit dysfunction (16), and dendritic spine morphology (17). Thus, the present study was undertaken to examine the hypothesis that aberrant ERK signaling outside of the hippocampus may contribute to synaptic phenotypes in fragile X mice.

Here we show that whereas mTOR signaling is elevated at synapses of the hippocampus (11), ERK (but not mTOR) signaling is elevated at synapses of the neocortex of *Fmr1* KO mice. We further show that phosphorylation of ribosomal protein S6, typically a target and downstream effector of mTOR, is elevated and lies downstream of ERK via the "alternative" S6 kinase p90-ribosomal S6 kinase (RSK), providing evidence of a noncanonical signaling pathway. Consistent with this, the brain-penetrant RSK inhibitor, BI-D1870, prevents audiogenic seizures, a hallmark feature of

Significance

Fragile X syndrome is the most common heritable cause of intellectual disability and autism. Elevated protein synthesis is considered a major contributor to the pathophysiology of fragile X. ERK (extracellular signal-regulated kinase) and mTOR (mechanistic target of rapamycin) are key signaling molecules in two prominent pathways that regulate protein synthesis. A major finding of this study is that ERK (but not mTOR) signaling is elevated in the neocortex of fragile X mice. Elevated ERK activity causes overactivation of p90-ribosomal S6 kinase (RSK) and hyperphosphorylation of ribosomal protein S6. Audiogenic seizures in fragile X mice, which mimic sensory hypersensitivity in fragile X humans, are prevented by RSK inhibition. Thus, RSK is a potential therapeutic target for treatment of fragile X.

Author contributions: K.S., A.P., M.V.L.B., and R.S.Z. conceived and designed research; K.S., A.P., and M.C., performed research, collected and assembled the data; K.S., A.P., M.C., M.V.L.B., and R.S.Z. analyzed and interpreted data; and K.S., A.P., M.C., M.V.L.B., and R.S.Z. wrote and approved the final manuscript.

Reviewers: L.K.K., Yale University School of Medicine; and S.J.L., Louisiana State University Health Sciences Center.

The authors declare no conflict of interest.

[1]K.S. and A.P. contributed equally to this work.

[2]Present address: Laboratory of Molecular Neuro-Oncology, The Rockefeller University, New York, NY 10065.

[3]To whom correspondence may be addressed. Email: ksawicka@rockefeller.edu, suzanne.zukin@einstein.yu.edu, or michael.bennett@einstein.yu.edu.

sensory hypersensitivity in fragile X mice. These findings provide evidence of disease-dependent alterations of the ERK/RSK signaling network in the neocortex of fragile X mice.

Results

ERK but Not mTOR Signaling Is Elevated in the Cortex of *Fmr1* KO Mice. Elevated protein synthesis is a hallmark feature of *Fmr1* KO mice (13, 18, 19). The ERK/MAPK and mTOR pathways are two critical signaling pathways that regulate protein synthesis in the brain and have been implicated in the pathophysiology of fragile X (3, 4). We focused on the neocortex, because neocortical network activity is enhanced in fragile X (20), and protein-synthesis–dependent synaptic plasticity is impaired in the fragile X cortex (21). ERK/MAPK signaling is initiated by activation of Ras, which phosphorylates the protein kinase MEK. We first examined the phosphorylation status and abundance of the upstream kinase MEK, which phosphorylates and activates ERK, in the neocortex of young fragile X mice. Phosphorylation of MEK at Ser217/221 showed a small yet significant increase, indicative of activation, in whole-cell lysates isolated from the neocortex of 4-wk-old *Fmr1* KO mice vs. wild-type littermates with little or no change in total MEK abundance (Fig. 1*A*). We next examined the phosphorylation status and abundance of the downstream target of MEK, ERK1/2, in young fragile X mice. Phosphorylation of ERK1/2 at Thr185/Tyr187 was elevated, indicative of activation, in whole-cell lysates from the neocortex of 4-wk-old *Fmr1* KO mice relative to that of control littermates, with little or no change in total ERK abundance (Fig. 1*B*).

To determine the downstream consequences of ERK activation, we focused on two downstream proteins, MAPK-interacting kinase 1 (MNK), which activates eukaryotic initiation factor-4E (eIF4E), and eIF4E, a protein essential for cap-dependent translation. Phosphorylation of MNK at Thr195/202 (Fig. 1*C*) and eIF4E at Ser209 (Fig. 1*D*) was elevated in whole-cell lysates from the neocortex of *Fmr1* KO mice vs. wild-type littermates at 4 wk of age, with little or no change in total MNK or total eIF4E abundance. Thus, elevated phosphorylation of MEK/ERK correlates with activation of two downstream targets of ERK, MNK and eIF4E, in the neocortex of young *Fmr1* KO mice.

We next examined the activity of the PI3K/Akt/mTOR pathway as assessed by the phosphorylation status of the PI3K effector the serine/threonine kinase Akt at Thr308, mTOR at Ser2448, and the mTOR complex 1 (mTORC1) substrate eIF4E-binding protein (4E-BP) at Thr37/46. Neither abundance nor phosphorylation of Akt at Thr308, mTOR at Ser2448, or 4E-BP at Thr37/46 was altered in whole-cell lysates from the neocortex of *Fmr1* KO mice relative to that of WT littermates at 4 wk of age (Fig. 1 *E*–*G*). Thus, ERK (but not mTOR) signaling is overactivated in the neocortex of 4-wk-old fragile X mice (Fig. 1*H*).

S6 Phosphorylation Is Elevated in Cortical Neurons via p90-RSK. Ribosomal protein S6 is a core component of the small ribosomal subunit that is essential to translation and is acutely phosphorylated in response to neuronal activity (22). S6 is directly phosphorylated by S6K, an established downstream target of mTOR, and its phosphorylation status is commonly considered a functional readout of mTOR activity (3). We examined whether S6 phosphorylation status and/or abundance was altered in the neocortex of 4-wk-old fragile X mice. Notably, whereas phosphorylation (and activation) of S6 at Ser235/236, an RSK- and S6K-dependent site, was markedly enhanced, phosphorylation of S6 at Ser240/44, an S6K-dependent yet RSK-independent site, was unaltered in the neocortex of fragile X vs. WT mice (Fig. 2*A*).

To determine the upstream kinase responsible for elevated S6 phosphorylation, we first examined the phosphorylation of S6 kinase. *Fmr1* KO mice exhibited a slight decrease in S6K phosphorylation at Thr389, with little or no difference in total abundance relative to that of control littermates (Fig. 2*B*). This finding is consistent with our finding that mTOR signaling is normal in the neocortex (above) and suggests that S6K is not the kinase responsible for hyperphosphorylation of S6. Although S6K is the best-known kinase to phosphorylate S6, an alternative family of serine/threonine kinases, termed the p90RSKs, which

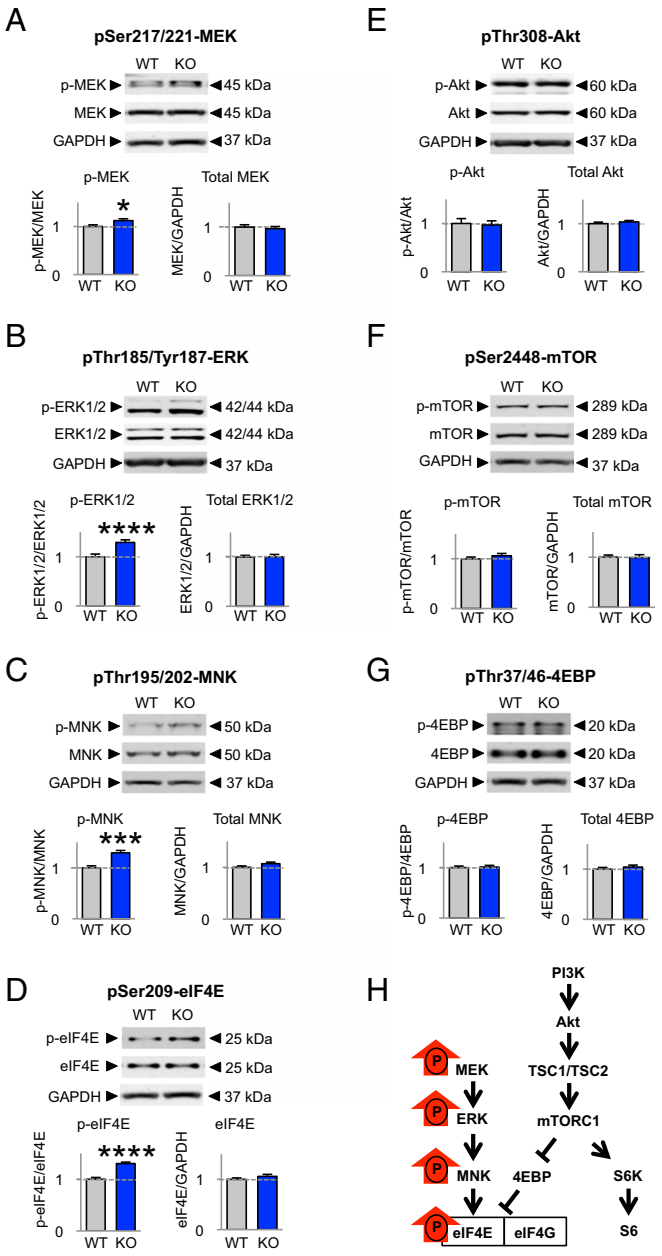

Fig. 1. MEK/ERK signaling, but not PI3K/mTOR signaling, is dysregulated in the neocortex of *Fmr1* KO mice. (*A*–*G*) Representative Western blots of cortical lysates from 4-wk-old WT and *Fmr1* KO mice and summary data showing relative abundance of phosphorylated and total protein. Western blots were probed for proteins in the ERK and mTOR pathways. Phosphorylation (but not total abundance) was elevated for proteins in the MEK/ERK pathway: p-MEK (WT, $n = 7$; KO, $n = 9$) (*A*), p-ERK (WT, $n = 22$; KO, $n = 24$) (*B*), p-MNK (WT, $n = 19$; KO, $n = 16$) (*C*), and p-eIF4E (WT, $n = 18$; KO, $n = 16$) (*D*). In contrast, there was no detectable difference in the phosphorylation status of proteins in the mTOR pathway: p-Akt (WT, $n = 5$; KO, $n = 6$) (*E*), p-mTOR (WT, $n = 7$; KO, $n = 9$) (*F*), and p-4EBP (WT, $n = 17$; KO, $n = 16$) (*G*). Data represent mean ± SEM; $^*P < 0.05$; $^{***}P < 0.001$; $^{****}P < 0.0001$. (*H*) Schematic of ERK and mTOR signaling in the neocortex of *Fmr1* KO mice depicting proteins with elevated basal phosphorylation (red arrows).

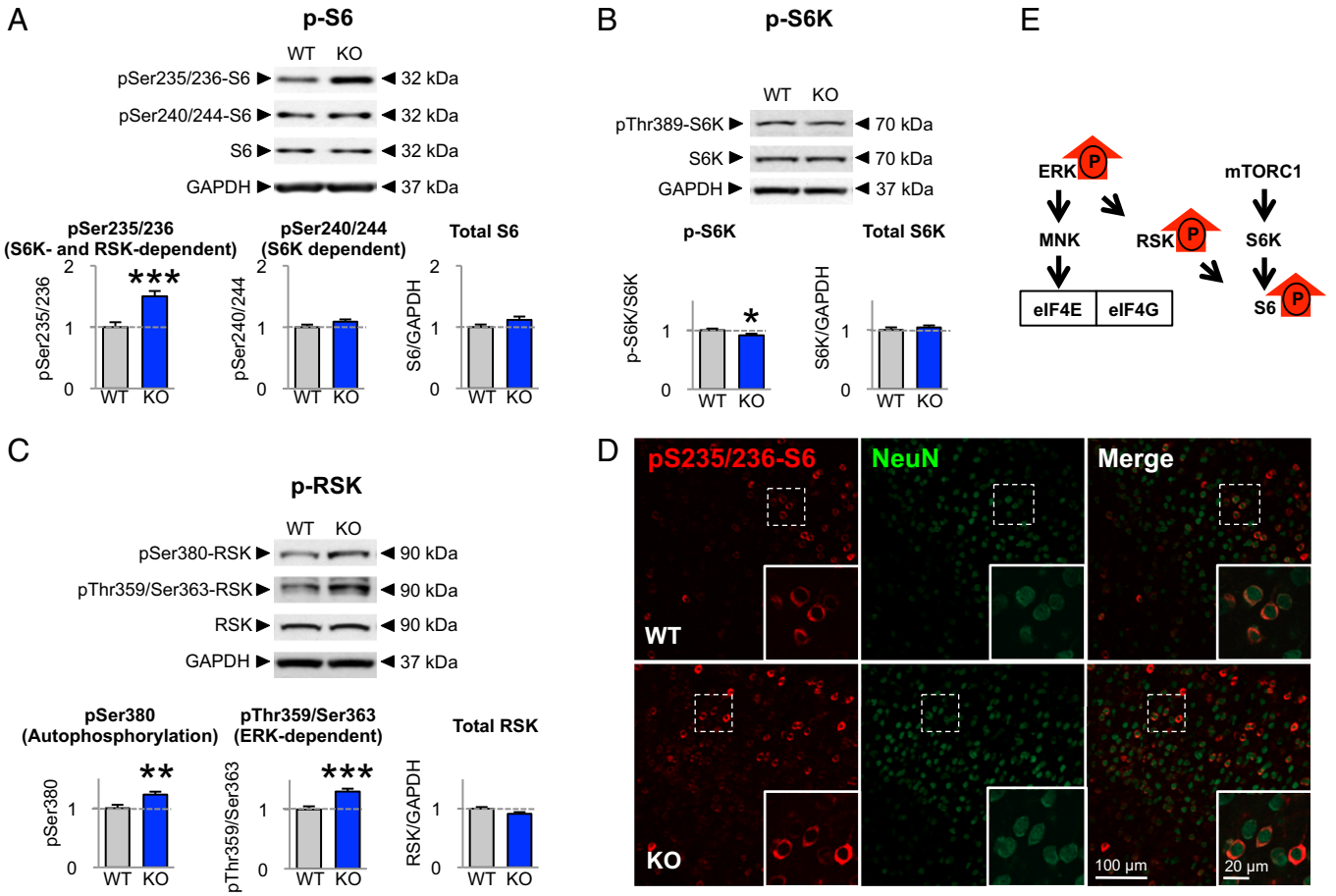

Fig. 2. Ribosomal protein S6 is phosphorylated in the cortex of *Fmr1* KO mice via RSK. (*A*–*C*) Representative Western blots of cortical lysates from WT and *Fmr1* KO mice and summary data showing relative abundance of phosphorylated and total protein levels. Whereas phosphorylation of S6 at Ser235/236, an RSK- and S6K-dependent site, was markedly enhanced (WT, $n = 16$; KO, $n = 15$), phosphorylation of S6 at Ser240/44, an S6K-dependent, RSK-independent site, was unaltered (WT, $n = 19$; KO, $n = 16$) in the neocortex of fragile X vs. WT mice (*A*). Whereas there was a slight decrease in the phosphorylation status of S6K (WT, $n = 19$; KO, $n = 16$) (*B*), there was a marked increase in the phosphorylation of RSK, at pT359/S363, the ERK-dependent phosphorylation site, and at S380, the autophosphorylation site (WT, $n = 19$; KO $n = 16$) (*C*). Data represent mean ± SEM; $^*P < 0.05$; $^{**}P < 0.01$; $^{***}P < 0.001$. (*D*) Immunofluorescence showing pS235/236-S6 (red) and the neuronal marker NeuN (green) in the somatosensory cortex of WT and KO mice. S6 phosphorylation was prominent in the soma of neurons. (*E*) Schematic of ERK/RSK/S6 signaling in the neocortex of *Fmr1* KO mice depicting proteins with elevated basal phosphorylation (red arrows).

lie downstream of ERK, can also phosphorylate S6 (23). The RSK family consists of four isoforms (RSK1–4) and is of particular interest in brain function because loss-of-function mutations in the *RPS6KA3* gene (gene encoding RSK2) cause Coffin–Lowry syndrome, an intellectual disability characterized by psychomotor deficits, digit and facial dysmorphisms, progressive skeletal deformations, and severe cognitive impairment (24). ERK directly phosphorylates RSK at several residues, including Thr359/Ser363 (25). ERK1/2-dependent phosphorylation and activation of RSK at Thr359/Ser363 within its carboxyl-terminal domain enable autophosphorylation of RSK at Ser380, which is critical for maximal RSK activity (26). Phosphorylation of RSK at Thr359/Ser363 (the ERK-dependent site), and at the autophosphorylation site Ser380, was elevated in the neocortex of fragile X vs. WT mice (Fig. 2*C*). In contrast, protein abundance was unchanged.

The results thus far indicate that S6 phosphorylation is elevated in cortical lysates of *Fmr1* KO mice but do not address the cell types in which this dysregulation occurs. To address this, we performed double immunofluorescence with a phospho-specific antibody to S6 phosphorylated at Ser235/236, in conjunction with an antibody to the neuronal marker NeuN in brain sections at the level of the neocortex of *Fmr1* KO mice and WT littermates (Fig. 2*D*). S6 phosphorylation was prominent in NeuN-positive cells and was elevated in sections from *Fmr1* KO vs. WT mice. These findings suggest that the increase in p-Ser235/236 detected in whole-tissue lysates occurs in neurons, but do not preclude the possibility that signaling is also altered in nonneuronal cells. Collectively, these findings are consistent with a model whereby overactivated ERK signaling induces elevated phosphorylation and activation of RSK, which phosphorylate S6 in an mTOR- and S6K-independent manner in the neocortex of fragile X mice (Fig. 2*E*).

Elevated ERK/RSK Signaling at Synapses Correlates with Increased Shank Phosphorylation. We next examined whether ERK/RSK/S6 signaling was dysregulated at cortical synapses of fragile X mice. Toward this end, we prepared cortical synaptoneurosomes from WT and *Fmr1* KO littermates. p-ERK, p-RSK, and p-S6 levels were elevated at cortical synapses of *Fmr1* KO mice with little or no change in protein abundance (Fig. 3 *A*–*C*). These findings provide evidence that elevated ERK/RSK signaling also occurs at the synapse.

In addition to its role in local protein synthesis via S6 phosphorylation, RSK is known to phosphorylate other substrates relevant to synaptic plasticity. Of particular interest is the Shank family of postsynaptic scaffolding and anchoring proteins implicated in autism spectrum disorders (27). Shank1 and Shank3 each contain

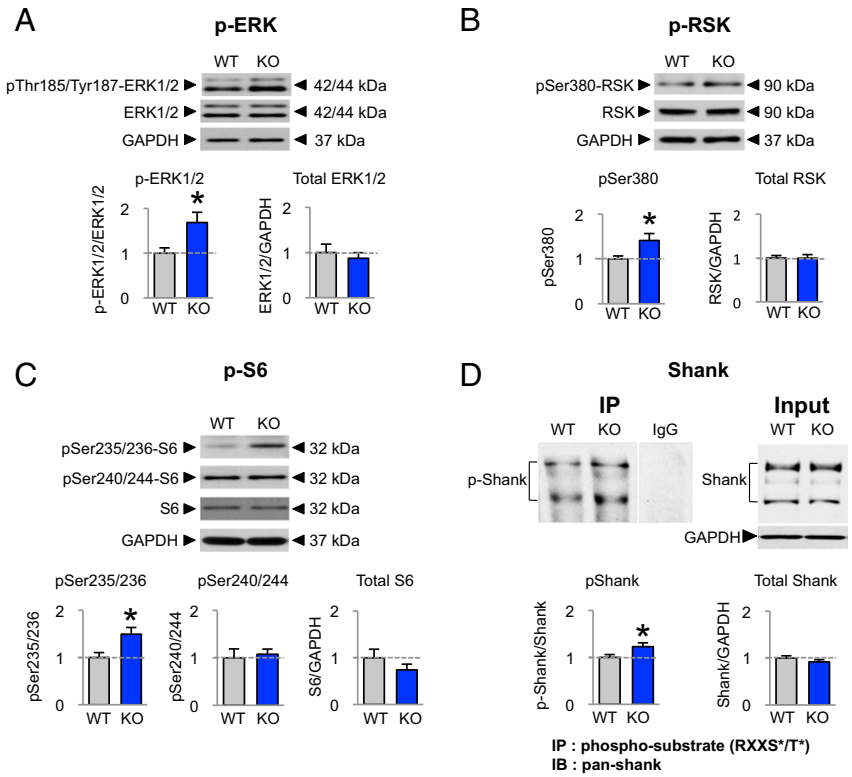

Fig. 3. ERK/RSK/S6 signaling and Shank phosphorylation are elevated at cortical synapses of *Fmr1* KO mice. (*A*–*C*) Representative Western blots of synaptosomes from the neocortex of WT and *Fmr1* KO mice and summary data showing relative abundance of phosphorylated and total ERK, RSK, and S6. Phosphorylation (but not total protein) was elevated for (*A*) p-ERK (WT, $n = 12$; KO, $n = 18$), (*B*) p-RSK (WT, $n = 8$; KO, $n = 15$), and (*C*) p-S6 at Ser235/236 (WT, $n = 9$; KO, $n = 17$), but not at Ser240/244 (WT, $n = 10$; KO, $n = 16$). (*D*) Phosphorylation of the RSK target Shank is increased in the synaptosomal fraction from neocortex of *Fmr1* KO mice. Phosphorylated proteins were immunoprecipitated from WT and KO synaptosomes by means of an antibody recognizing the RSK phospho-motif (phospho-RXXS*/T*). Western blots using an antibody recognizing all forms of Shank were used on the immunoprecipitate (IP) and input of synaptosomal proteins of the WT and *Fmr1* KO mice. There was no detectable change in the levels of Shank in the input between WT and KO but there was significant increase in the amount of Shank immunoprecipitated by the phospho-specific antibody, indicating elevated Shank phosphorylation at the RSK motif (WT, $n = 17$; KO, $n = 15$). Data represent mean ± SEM; $^*P < 0.05$.

several RSK consensus phosphorylation sites (RXRXXS, where X is any amino acid) (28). We reasoned that overactivated RSK might induce elevated Shank phosphorylation. The sites at which RSK phosphorylates and activates Shank are, as yet, unknown and currently no phospho-specific antibody is commercially available. We therefore used a strategy that uses an antibody recognizing the RSK phospho-motif (phospho-RXXS*/T*). We prepared synaptosomes from the neocortex of WT and *Fmr1* KO mice and performed immunoprecipitation with an antibody against the RSK phospho-motif, followed by Western blots probed with a (pan) anti-Shank antibody. The proportion of Shank that immunoprecipitated with the antibody to the RSK phospho-motif, relative to that in the input, was significantly increased in synaptosomes from *Fmr1* KO mice, indicative of enhanced RSK-dependent phosphorylation of Shank at cortical synapses of *Fmr1* KO mice (Fig. 3*D*). These findings indicate that elevated RSK activity at cortical synapses of fragile X mice is associated with elevated phosphorylation of its downstream target Shank, which may be related to dysregulated synaptic scaffolds and synaptic transmission.

Adult Fragile X Mice Exhibit Persistent Dysregulation of ERK/RSK Signaling. Because the fragile X phenotype arises in early childhood and persists into adulthood, we next examined whether dysregulated ERK/RSK signaling persists into adulthood in fragile X mice. p-MEK, p-ERK, p-MNK, p-eIF4E, and p-RSK were elevated in adult (10-wk-old) fragile X mice, indicative of persistent elevation of ERK/RSK signaling (Fig. 4 *A*–*E*). Importantly, only the RSK-dependent phosphorylation site of p-S6 (Ser235/236) but not the S6K-dependent site (Ser240/44) was elevated in adult fragile X neocortex (Fig. 4*F*), consistent with the concept that ERK/RSK (but not mTOR) signaling is dysregulated in the neocortex of fragile X mice (Fig. 4*G*).

Inhibition of ERK Signaling Rescues Elevated eIF4E, RSK, and S6 Phosphorylation. The results thus far demonstrate that ERK/RSK signaling and S6 phosphorylation are elevated in whole-cell lysates and synaptosomes from the neocortex of fragile X mice but do not address a causal relation between them. To address this issue, we examined whether acute pharmacological inhibition of MEK/ERK signaling could effectively reduce the elevated phosphorylation of RSK and S6 seen in the *Fmr1* KO neocortex. We administered the brain-penetrant MEK inhibitor SL327 (100 mg/kg, i.p., 60 min before killing) to *Fmr1* KO mice and measured the phosphorylation status of two downstream targets of mTOR, S6K at Thr389 and 4EBP at Thr37/46 (Fig. 5 *A* and *B*). SL327 induced no detectable change in the phosphorylation status or protein abundance of either S6K or 4EBP in cortical lysates from SL327-treated vs. vehicle-treated mice of either genotype. These findings are consistent with the lack of effect of the MEK-selective inhibitor on mTOR activity. In contrast, a single, acute injection of SL327 reduced the phosphorylation status of ERK to almost undetectable levels with no change in total ERK protein, indicating effective inhibition of MEK in the neocortex (Fig. 5*C*).

The MEK inhibitor SL327 markedly reduced elevated p-eIF4E in cortical lysates from *Fmr1* KO mice to that of WT levels with little or no effect on total eIF4E abundance (Fig. 5*D*). By

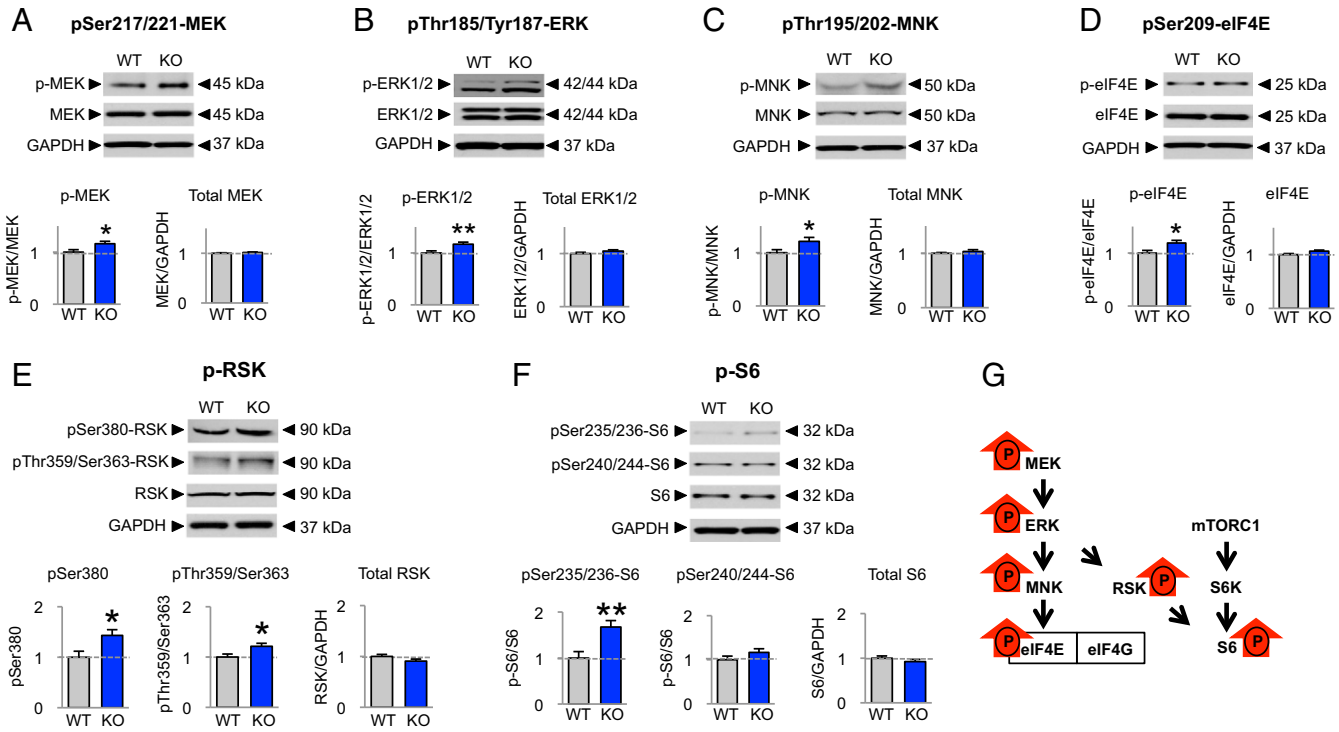

Fig. 4. Adult fragile X mice display elevated ERK/RSK/S6 signaling in the neocortex. (*A–F*) Representative Western blots of cortical lysates from 10-wk-old WT and *Fmr1* KO littermates and summary data showing relative abundance of phosphorylated and total protein. Western blots were probed for proteins in the ERK/RSK/S6 pathway. Phosphorylation (but not total abundance) was elevated for proteins in the ERK pathway: (*A*) p-MEK (WT, $n = 16$; KO, $n = 13$), (*B*) p-ERK (WT, $n = 14$; KO, $n = 16$), (*C*) p-MNK (WT, $n = 22$; KO, $n = 22$), (*D*) p-eIF4E (WT, $n = 18$; KO, $n = 16$), (*E*) p-RSK (WT, $n = 12$; KO, $n = 10$), and (*F*) p-S6 (WT, $n = 12$; KO, $n = 9$). Data represent mean ± SEM; $*P < 0.05$; $**P < 0.01$. (*G*) Schematic of the ERK and mTOR signaling in the neocortex of *Fmr1* KO mice.

contrast, SL327 had little or no effect on the phosphorylation status or abundance of eIF4E in cortical lysates from WT mice. These findings indicate that whereas elevated p-eIF4E in the *Fmr1* KO mouse is acutely dependent on ERK activity, normal eIF4E phosphorylation in WT mice was stable to 1 h exposure to SL327. In addition to its actions on eIF4E, SL327 markedly reduced ERK-dependent phosphorylation of RSK at Thr359/Ser363 and autophosphorylation of RSK at Ser380 in the neocortex of both WT and *Fmr1* KO animals (Fig. 5*E*). These data demonstrate that elevated RSK activity in the *Fmr1* KO neocortex can be rapidly corrected by acute pharmacological inhibition of MEK and indicate that the elevated RSK activity observed in *Fmr1* KO neocortex is downstream of overactivated ERK/MAPK signaling.

Acute pharmacological inhibition of MEK by SL327 reduced elevated S6 phosphorylation in the fragile X neocortex, but had little or no effect on S6 phosphorylation in WT neocortex (Fig. 5*F*). This finding confirms that S6 lies downstream of MEK in the *Fmr1* KO neocortex and is acutely sensitive to ERK activity. Notably S6 phosphorylation was not changed despite changes to p-RSK in WT mice, suggesting that RSK-dependent regulation of S6 is restricted to *Fmr1* KO mice. Collectively these findings demonstrate a causal relation between elevated ERK/RSK signaling and elevated S6 activity in fragile X mice.

Inhibition of RSK Prevents Audiogenic Seizures in Fragile X Mice. ERK signaling is implicated in the pathophysiology of fragile X mice (14). Because aberrant ERK/MAPK is causally related to elevated RSK activity in *Fmr1* KO neocortex, we examined whether direct inhibition of RSK (which lies downstream of ERK/MAPK) could rescue, at least in part, a behavioral fragile X phenotype. Audiogenic seizures are a hallmark behavior observed in fragile X mice and are thought to mimic the sensory hypersensitivity observed in humans with fragile X syndrome (20). A 130-dB siren elicited a robust audiogenic seizure in nontreated and vehicle-injected fragile X mice (Fig. 6 *A* and *B*). Acute administration of the blood–brain-permeable RSK inhibitor, BI-D1870 (50 mg/kg, 60 min before testing), prevented the seizures in fragile X mice (Fig. 6*B*). These findings suggest that elevated RSK activity contributes, at least in part, to the seizure susceptibility observed in fragile X mice, although we cannot rule out the possibility that BI-D1870 is acting on other pathways (29).

Discussion

Excessive protein synthesis is a molecular hallmark of fragile X mice and is implicated in the impaired protein synthesis-dependent synaptic plasticity observed at synapses of the neocortex and hippocampus. ERK signaling and mTOR signaling are two prominent pathways known to regulate protein synthesis. A major finding of the present study is that ERK, but not mTOR, signaling is elevated in the neocortex of young fragile X mice. Moreover, we show that phosphorylation of ribosomal protein S6, typically a downstream target and key effector of mTOR, is elevated and lies downstream of ERK via the alternative S6 kinase RSK, as evidenced by findings that a MEK/ERK inhibitor reduces elevated S6 phosphorylation and activation. These results are significant in that S6 facilitates gene expression, translation, cell growth, and proliferation in an activity-dependent manner. The alterations in signaling networks in the *Fmr1* KO neocortex may account for the excessive protein synthesis, spine dysmorphogenesis, and impaired protein-synthesis–dependent synaptic plasticity.

Our observation of elevated ERK signaling in the neocortex of fragile X mice differs from those of others, who show that ERK signaling is normal in the hippocampus and neocortex (10, 14). We expect that differences in the techniques used are responsible

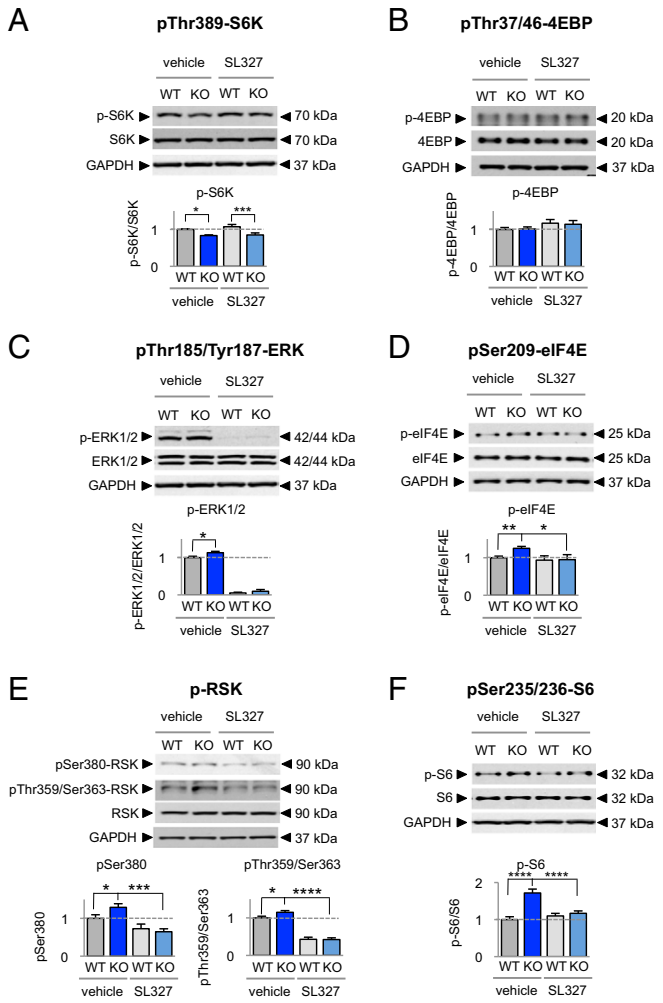

Fig. 5. Inhibition of ERK signaling rescues elevated eIF4E, RSK, and S6 phosphorylation. WT and *Fmr1* KO mice were injected i.p. with 100 mg/mL SL327 or vehicle (60% DMSO/40% saline) and killed 60 min after treatment. Representative Western blots and summary data are shown. (*A*) SL327 had little or no effect on phosphorylation status or abundance of the mTOR downstream effector S6K ($n = 10$ per group). (*B*) Similarly, pThr37/46-4EBP was little affected in the WT or KO with or without SL327 treatment ($n = 4$ per group). (*C*) SL327 effectively inhibited ERK phosphorylation in WT and *Fmr1* KO mice ($n = 10$ per group). (*D*) SL327 restored phosphorylation of eIF4E to WT levels ($n = 9$–10 per group). (*E*) SL327 reduced RSK phosphorylation in WT and KO at the ERK and autophosphorylation sites and corrected the difference between WT and KO levels (pT359/S363 RSK, $n = 5$ per group; p-S380 RSK, $n = 8$–10 per group). (*F*) SL327 rescued elevated phosphorylation of S6 in *Fmr1* KO mice, with little or no effect in WT mice (pS235/236-S6, $n = 7$–8 per group). Data represent mean ± SEM; $^{*}P < 0.05$; $^{**}P < 0.01$; $^{***}P < 0.001$; $^{****}P < 0.0001$.

and think that ours are more reliable. The present study provides an advance over previous studies in that we show dysregulation of MEK, ERK, MNK, eIF4E, RSK, and S6 in the neocortex of fragile X mice and a causal relation between elevated ERK/RSK signaling and S6 overactivation. Findings in the present study show that elevated ERK/RSK signaling in the neocortex contributes to seizure susceptibility. It has been shown that the MEK inhibitor SL327 can prevent audiogenic seizures in fragile X mice (14). Here we demonstrate that the RSK inhibitor, BI-D1870, also prevents audiogenic seizures, suggesting that block of downstream RSK signaling is the mechanism whereby MEK/ERK inhibition prevents the seizures.

A finding of the present study is that elevated RSK signaling leads to hyperphosphorylation of Shank, a protein implicated in AMPAR receptor function, spine stabilization, and synaptic plasticity (30, 31). Shank family proteins (Shank1–3) are synaptic scaffolding proteins critical to the organization and structure of the postsynaptic density of excitatory glutamatergic synapses. RSK2 has been shown to interact with the PDZ domain of Shank proteins and phosphorylate both Shank1 and Shank3, a step critical to normal AMPAR synaptic transmission (30, 31). Human genetic studies as well as studies using mouse models have identified mutations in the Shank genes as causative of synaptic dysfunction and autism-relevant behaviors (32). Given the importance of Shank in other forms of autism, our data suggest that dysregulation of RSK and thus Shank function may be associated with other autism spectrum disorders (ASDs) as well as fragile X.

Ribosomal protein S6 is a convergence point of ERK and mTOR signaling to control protein synthesis (26). An important finding of this paper is that the MEK inhibitor SL327, which significantly reduces RSK activity in the neocortex of both WT and KO mice, corrects elevated S6 phosphorylation in fragile X mice with little to no effect on S6 activity in WT animals. This suggests that, in WT animals, S6 primarily receives input from mTOR via S6K whereas, in fragile X, S6 acquires disease-relevant input from ERK via RSK.

ASDs are a diverse group of developmental disorders, characterized by deficits in social interactions, impairments in communication, and repetitive and stereotypic behaviors (32). Although ASDs can arise as a consequence of mutations, deletions, or duplications of a number of genes with differing molecular functions, they appear to converge on common biological pathways to give rise to autism-relevant behaviors (33). One such pathway is the mTOR pathway (34). Findings in the present study suggest that ERK/RSK signaling may be another common mechanism whereby RSK overactivation contributes to the pathophysiology observed in fragile X and potentially other ASDs. An example is Coffin–Lowry syndrome, which is a syndromic form of X-linked intellectual disability caused by a loss-of-function mutation of the *RPS6KA3* gene (encoding RSK2), characterized by psychomotor deficits, digit and facial dysmorphisms, progressive skeletal deformations, and severe cognitive impairments (24). RSK2 plays an important role in a negative feedback loop that inhibits the Raf/MEK/ERK/RSK pathway (35). Interestingly, RSK2 mutant mice exhibit unchecked

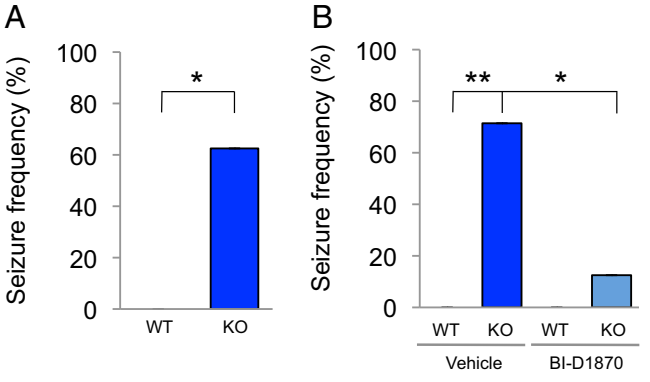

Fig. 6. RSK inhibition prevents audiogenic seizures in *Fmr1* KO mice. (*A*) Five of eight untreated *Fmr1* KO mice exposed twice to a 130-dB siren for 2 min displayed audiogenic seizures, whereas untreated WT mice ($n = 9$) did not. (*B*) WT and *Fmr1* KO mice were injected i.p. with 5 mg/mL BI-D1870 or vehicle (1.5% Solutol in 60% DMSO/40% saline) and assessed for audiogenic seizures 60 min after drug administration. RSK inhibition reduced susceptibility to audiogenic seizures in *Fmr1* KO mice. Five of seven vehicle-injected *Fmr1* KO mice had seizures; one of eight BI-D1870–treated *Fmr1* KO mice had a seizure (Fisher's exact tests; $^{*}P < 0.05$; $^{**}P < 0.01$).

MEK/ERK/RSK signaling presumably due to elevated RSK1 and/or RSK3 activity in the hippocampus (36), which is accompanied by impaired spatial learning and memory, stereotypy, and increased exploratory behavior (37). This suggests that elevated ERK/RSK signaling may promote autism-relevant behaviors. Accordingly, in our study we show that ERK/RSK signaling is enhanced in fragile X and dampening ERK/RSK signaling reduces audiogenic seizures in fragile X mice, making RSK a potential therapeutic target for the amelioration of cognitive defects in individuals with fragile X.

Materials and Methods

Animals. WT and *Fmr1* KO mice on the C57BL/6 genetic background were a kind gift from E. Klann, New York University, NY. Animals were maintained in a temperature- and light-controlled environment with a 12:12-h light: dark cycle and were treated in accordance with the principles and procedures of the National Institutes of Health Guidelines for the Care and Use of Laboratory Animals. Protocols were approved by the Institutional Animal Care and Use Committee of the Albert Einstein College of Medicine. Unless stated otherwise, animals used for these studies were male littermates killed at P28–32 by an overdose of isoflurane and decapitation.

Western Blotting. Western blotting was performed as described in ref. 38. Brains were removed and the neocortex was rapidly dissected in ice-cold homogenization buffer (320 mM sucrose, 1 mM EDTA, 5 mM Tris, pH 7.4; 0.25 mM DTT and protease and phosphatase inhibitors were added immediately before use). The cortex was immediately homogenized with 20 strokes of a Dounce homogenizer and either snap frozen in liquid nitrogen or processed for synaptosome fractionation. For Western blots of total lysates, homogenates were lysed in 2 vol of lysis buffer [25 mM Tris (pH 7.4), 150 mM NaCl, 1 mM EDTA (pH 8.0), 0.1% SDS, 0.5% sodium deoxycholate, 1% Triton X-100 with protease and phosphatase inhibitors] and sonicated. Protein concentration was determined by means of a BCA protein assay kit (Pierce). Aliquots (20–30 μg) were run on NuPAGE gels (Invitrogen), transferred to a nitrocellulose membrane, and probed with antibody. Band densities were measured using ImageJ software. Results were normalized within each litter before comparison across multiple litters. Each litter used contained a minimum of one WT and one KO male.

Immunofluorescence. Animals were perfused with PBS followed by ice-cold 4% (wt/vol) paraformaldehyde in PBS. Brains were removed, fixed in 4% (wt/vol) paraformaldehyde at 4 °C overnight, incubated in 30% (wt/vol) sucrose in PBS at 4 °C for 48 h, and then frozen at −80 °C. Coronal sections (20 μm) were cut with a cryotome. Immunofluorescence was carried out with free-floating sections. Sections were permeabilized in 0.2% Triton and blocked with blocking buffer [10% (vol/vol) normal goat serum, 0.05% Triton, PBS]. Sections were incubated first with p-S235/236 S6 antibody (1:200; Cell Signaling) in antibody dilution buffer (1% BSA, 0.05% Triton, PBS) overnight at 4 °C and then for 2 h at room temperature with NeuN antibody (1:1,000; Millipore). Sections were incubated for 1 h at room temperature with goat anti-mouse Alexa Fluor 488 and goat anti-rabbit Alexa Fluor 546 antibodies (Invitrogen), washed, and mounted with Vectashield mounting medium. Sections were imaged using a Zeiss LSM510 confocal microscope.

Drug Injections. To minimize the effect of stress from the injections (39, 40), the animals were acclimated to i.p. injections for 3 d before the experiment. During this time the animals were acclimated to the transport, weighing, and handling and received a single i.p. injection of 0.9% saline each day for 3 d. For ERK inhibition, on the fourth day the animals received 100 mg/kg SL327 (dissolved at 30 mg/mL in vehicle) or vehicle alone (60% DMSO/40% saline) and were returned to the home cage. The mice were killed and the cortex was dissected 60 min after injection. For RSK inhibition animals received 50 mg/kg BI-D1870 [dissolved at 5 mg/mL in vehicle (41)] or vehicle alone [1.5% (wt/vol) Solutol in 60% DMSO/40% saline] and were returned to the home cage. Sixty minutes after injection mice were tested for audiogenic seizures.

Synaptosome Fractionation. Synaptosomes were prepared as previously described (42). In brief, homogenates were centrifuged at 1,000 × *g* (10 min at 4 °C) and supernatants were loaded onto a discontinuous Percoll gradient. After centrifugation at 31,000 × *g* (6 min at 4 °C) with a JA-20 rotor, synaptosomes were collected from the 15% (vol/vol)–23% (vol/vol) Percoll interface, diluted in PBS, and pelleted by centrifugation at 20,000 × *g* for 10 min. Synaptosomes were lysed in lysis buffer and processed for Western blotting as described above.

Immunoprecipitation. Tissue was homogenized in 3 mL IP homogenization buffer (320 mM sucrose, 4 mM Hepes, pH 7.3, with protease and phosphatase inhibitors) in a Dounce homogenizer. Homogenates were centrifuged at 900 × *g* for 10 min at 4 °C and the supernatant was spun again at 900 × *g* for an additional 10 min. The supernatant was centrifuged at 13,000 × *g* for 15 min at 4 °C to pellet the P2 crude synaptosome fraction. The P2 pellet was resuspended in IP buffer (50 mM Tris, pH 7.4, 0.1 mM EGTA, 0.1% Triton containing protease and phosphatase inhibitors) and solubilized for 20 min with rotation at 4 °C, and the insoluble material was removed by centrifugation at 20,000 × *g* (15 min at 4 °C). Protein A/G agarose beads (25 μL per sample; Santa Cruz) were precoated with phospho-RXXS*/T* antibody (1 μg/25 μL beads; Cell Signaling) or normal rabbit IgG (Santa Cruz) by incubation with rotation overnight in PBS at 4 °C and washed in IP buffer. A total of 500 μg solubilized P2 fraction was incubated with precoated beads (2 h at 4 °C) and the beads were washed five times with IP buffer. Protein was eluted from the beads by heating (10 min at 95 °C) in loading buffer [50 mM Tris, pH 6.8, 10% (vol/vol) glycerol, 4% (wt/vol) SDS, 10% (vol/vol) β-mercaptoethanol, 1 mM EDTA, bromophenol blue].

Audiogenic Seizures. Audiogenic seizures were induced as described in ref. 14. P19–P24 WT and *Fmr1* KO mice were placed in a plastic chamber containing a 130-dB siren (PAL-1 Personal Alarm) covered with a plastic lid. Animals were subjected to habituation (1 min), followed by exposure to the siren (2 min), silence (1 min), and additional exposure to the siren (2 min). Mice were videotaped and scored.

Antibodies. The following antibodies were used in this study: p-MEK (1:1,000; Cell Signaling, 9154S), MEK (1:1,000; Cell Signaling, 8727S), p-ERK (1:1,000; Cell Signaling, 4370S), ERK (1:3,000; Millipore, 06–182), p-MNK (1:1,000; Cell Signaling, 2111S), MNK (1:1,000; Cell Signaling, 2195S), p-eIF4E (1:1,000; Cell Signaling, 9741S), eIF4E (1:1,000; Cell Signaling, 2067S), p-mTOR (1:1,000; Cell Signaling, 2971L), mTOR (1:1,000; Cell Signaling, 4517S), p-Akt (1:1,000; Cell Signaling, 2965S), Akt (1:1,000; Cell Signaling, 9272S), p-4E-BP (1:1,000; Cell Signaling, 9459S), 4E-BP (1:1,000; Cell Signaling, 9644S), p-S6K1 (1:1,000; Cell Signaling, 2708S), S6K1 (1:1,000; Cell Signaling, 9206S), pSer235/236 S6 (1:1,000 for Western blots and 1:500 for immunofluorescence; Cell Signaling, 4858S), pSer240/244 S6 (1:1,000; Cell Signaling, 5364S), S6 (1:1,000; Cell Signaling, 2317S), pSer380 RSK (1:1,000; Cell Signaling, 9335S), pT359/S363 RSK (1:1,000; Cell Signaling, 9344S), RSK1/2/3 (1:1,000; Cell Signaling, 9355S), Pan-Shank (1:1,000; NeuroMab, 75-089), NeuN (1:1,000; Millipore, MAB377) GAPDH (1:50,000; Fitzgerald, 10R-G109A), HRP-linked mouse IgG (1:5,000; Cell Signaling, 7076S), and HRP-linked rabbit IgG (1:5,000; Cell Signaling, 7074S).

Statistical Analysis. Data analysis was performed by means of GraphPad Prism 6.00. Statistics were calculated using Student's unpaired, two-tailed *t* test. In the case of more than two groups, one-way ANOVA was used with post hoc Student's unpaired, two-tailed *t* test for pairwise comparisons. Two-tailed Fisher's exact test was used for audiogenic seizures. Statistical significance was defined as $P < 0.05$.

ACKNOWLEDGMENTS. We thank Fabrizio Pontarelli and Brenda Court-Vasquez for technical assistance and Dr. Jingqi Yan for invaluable advice. We thank members of the R.S.Z. laboratory for helpful comments and suggestions on the manuscript. This work was supported by NIH Grants MH092877 and NS45693, a McKnight Foundation Brain Disorders Award, a National Association for Research on Schizophrenia and Depression Distinguished Investigator Award from the Brain & Behavior Research Foundation, a generous grant from the F. M. Kirby Foundation (to R.S.Z.), and a FRAXA Research Foundation Postdoctoral Fellowship (to K.S.). R.S.Z. is the F. M. Kirby Professor in Neural Repair and Protection.

1. Wadell PM, Hagerman RJ, Hessl DR (2013) Fragile X syndrome: Psychiatric manifestations, assessment and emerging therapies. *Curr Psychiatry Rev* 9(1):53–58.
2. Darnell JC, et al. (2011) FMRP stalls ribosomal translocation on mRNAs linked to synaptic function and autism. *Cell* 146(2):247–261.
3. Richter JD, Bassell GJ, Klann E (2015) Dysregulation and restoration of translational homeostasis in fragile X syndrome. *Nat Rev Neurosci* 16(10):595–605.
4. Kelleher RJ, 3rd, Bear MF (2008) The autistic neuron: Troubled translation? *Cell* 135(3): 401–406.
5. Lüscher C, Huber KM (2010) Group 1 mGluR-dependent synaptic long-term depression: Mechanisms and implications for circuitry and disease. *Neuron* 65(4): 445–459.
6. Qin M, Kang J, Burlin TV, Jiang C, Smith CB (2005) Postadolescent changes in regional cerebral protein synthesis: An in vivo study in the FMR1 null mouse. *J Neurosci* 25(20): 5087–5095.
7. Dölen G, et al. (2007) Correction of fragile X syndrome in mice. *Neuron* 56(6): 955–962.

8. Gross C, Bassell GJ (2012) Excess protein synthesis in FXS patient lymphoblastoid cells can be rescued with a p110β-selective inhibitor. *Mol Med* 18:336–345.
9. Darnell JC, Klann E (2013) The translation of translational control by FMRP: Therapeutic targets for FXS. *Nat Neurosci* 16(11):1530–1536.
10. Gross C, et al. (2010) Excess phosphoinositide 3-kinase subunit synthesis and activity as a novel therapeutic target in fragile X syndrome. *J Neurosci* 30(32):10624–10638.
11. Sharma A, et al. (2010) Dysregulation of mTOR signaling in fragile X syndrome. *J Neurosci* 30(2):694–702.
12. Bhattacharya A, et al. (2012) Genetic removal of p70 S6 kinase 1 corrects molecular, synaptic, and behavioral phenotypes in fragile X syndrome mice. *Neuron* 76(2): 325–337.
13. Gross C, et al. (2015) Increased expression of the PI3K enhancer PIKE mediates deficits in synaptic plasticity and behavior in fragile X syndrome. *Cell Rep* 11(5):727–736.
14. Osterweil EK, Krueger DD, Reinhold K, Bear MF (2010) Hypersensitivity to mGluR5 and ERK1/2 leads to excessive protein synthesis in the hippocampus of a mouse model of fragile X syndrome. *J Neurosci* 30(46):15616–15627.
15. Li J, Pelletier MR, Perez Velazquez JL, Carlen PL (2002) Reduced cortical synaptic plasticity and GluR1 expression associated with fragile X mental retardation protein deficiency. *Mol Cell Neurosci* 19(2):138–151.
16. Paluszkiewicz SM, Olmos-Serrano JL, Corbin JG, Huntsman MM (2011) Impaired inhibitory control of cortical synchronization in fragile X syndrome. *J Neurophysiol* 106(5):2264–2272.
17. He CX, Portera-Cailliau C (2013) The trouble with spines in fragile X syndrome: Density, maturity and plasticity. *Neuroscience* 251:120–128.
18. Guo W, Ceolin L, Collins KA, Perroy J, Huber KM (2015) Elevated CaMKIIα and hyperphosphorylation of Homer mediate circuit dysfunction in a Fragile X syndrome mouse model. *Cell Rep* 13(10):2297–2311.
19. Michalon A, et al. (2012) Chronic pharmacological mGlu5 inhibition corrects fragile X in adult mice. *Neuron* 74(1):49–56.
20. Contractor A, Klyachko VA, Portera-Cailliau C (2015) Altered neuronal and circuit excitability in fragile X syndrome. *Neuron* 87(4):699–715.
21. Chen T, et al. (2014) Pharmacological rescue of cortical synaptic and network potentiation in a mouse model for fragile X syndrome. *Neuropsychopharmacology* 39(8):1955–1967.
22. Knight ZA, et al. (2012) Molecular profiling of activated neurons by phosphorylated ribosome capture. *Cell* 151(5):1126–1137.
23. Roux PP, et al. (2007) RAS/ERK signaling promotes site-specific ribosomal protein S6 phosphorylation via RSK and stimulates cap-dependent translation. *J Biol Chem* 282(19):14056–14064.
24. Pereira PM, Schneider A, Pannetier S, Heron D, Hanauer A (2010) Coffin-Lowry syndrome. *Eur J Hum Genet* 18(6):627–633.
25. Lara R, Seckl MJ, Pardo OE (2013) The p90 RSK family members: Common functions and isoform specificity. *Cancer Res* 73(17):5301–5308.
26. Anjum R, Blenis J (2008) The RSK family of kinases: Emerging roles in cellular signalling. *Nat Rev Mol Cell Biol* 9(10):747–758.
27. Sala C, Vicidomini C, Bigi I, Mossa A, Verpelli C (2015) Shank synaptic scaffold proteins: Keys to understanding the pathogenesis of autism and other synaptic disorders. *J Neurochem* 135(5):849–858.
28. Leighton IA, Dalby KN, Caudwell FB, Cohen PT, Cohen P (1995) Comparison of the specificities of p70 S6 kinase and MAPKAP kinase-1 identifies a relatively specific substrate for p70 S6 kinase: The N-terminal kinase domain of MAPKAP kinase-1 is essential for peptide phosphorylation. *FEBS Lett* 375(3):289–293.
29. Neise D, et al. (2013) The p90 ribosomal S6 kinase (RSK) inhibitor BI-D1870 prevents gamma irradiation-induced apoptosis and mediates senescence via RSK- and p53-independent accumulation of p21WAF1/CIP1. *Cell Death Dis* 4:e859.
30. Sala C, et al. (2001) Regulation of dendritic spine morphology and synaptic function by Shank and Homer. *Neuron* 31(1):115–130.
31. Thomas GM, Rumbaugh GR, Harrar DB, Huganir RL (2005) Ribosomal S6 kinase 2 interacts with and phosphorylates PDZ domain-containing proteins and regulates AMPA receptor transmission. *Proc Natl Acad Sci USA* 102(42):15006–15011.
32. de la Torre-Ubieta L, Won H, Stein JL, Geschwind DH (2016) Advancing the understanding of autism disease mechanisms through genetics. *Nat Med* 22(4):345–361.
33. Sawicka K, Zukin RS (2012) Dysregulation of mTOR signaling in neuropsychiatric disorders: Therapeutic implications. *Neuropsychopharmacology* 37(1):305–306.
34. Huber KM, Klann E, Costa-Mattioli M, Zukin RS (2015) Dysregulation of mammalian target of rapamycin signaling in mouse models of autism. *J Neurosci* 35(41): 13836–13842.
35. Kim M, et al. (2006) Inhibition of ERK-MAP kinase signaling by RSK during Drosophila development. *EMBO J* 25(13):3056–3067.
36. Schneider A, Mehmood T, Pannetier S, Hanauer A (2011) Altered ERK/MAPK signaling in the hippocampus of the mrsk2_KO mouse model of Coffin-Lowry syndrome. *J Neurochem* 119(3):447–459.
37. Poirier R, et al. (2007) Deletion of the Coffin-Lowry syndrome gene Rsk2 in mice is associated with impaired spatial learning and reduced control of exploratory behavior. *Behav Genet* 37(1):31–50.
38. Rodenas-Ruano A, Chávez AE, Cossio MJ, Castillo PE, Zukin RS (2012) REST-dependent epigenetic remodeling promotes the developmental switch in synaptic NMDA receptors. *Nat Neurosci* 15(10):1382–1390.
39. Meller E, et al. (2003) Region-specific effects of acute and repeated restraint stress on the phosphorylation of mitogen-activated protein kinases. *Brain Res* 979(1–2):57–64.
40. Yang PC, Yang CH, Huang CC, Hsu KS (2008) Phosphatidylinositol 3-kinase activation is required for stress protocol-induced modification of hippocampal synaptic plasticity. *J Biol Chem* 283(5):2631–2643.
41. Pambid MR, et al. (2014) Overcoming resistance to Sonic Hedgehog inhibition by targeting p90 ribosomal S6 kinase in pediatric medulloblastoma. *Pediatr Blood Cancer* 61(1):107–115.
42. Dunkley PR, Jarvie PE, Robinson PJ (2008) A rapid Percoll gradient procedure for preparation of synaptosomes. *Nat Protoc* 3(11):1718–1728.